Corrosion mitigation by an eco-friendly inhibitor: *Beta vulgaris* (beetroot) extract on mild steel in simulated oil well water medium

S.C. Joycee,[1,2] A.S. Raja,[2] A.S. Amalraj[3] and S. Rajendran[1,4]*

[1]*Department of Chemistry, Corrosion Research Centre, St. Antony's College of Arts and Sciences for Women, Dindigul-624 005, India*
[2]*Department of Chemistry, G.T.N Arts College (Autonomous), Dindigul-624 005, India*
[3]*Department of Physics, Sree Sevugan Annamalai College, Devakottai-630 303, India*
[4]*Adjunct Professor, Pondicherry University, Puducherry, India*
**E-mail: susairajendran@gmail.com*

Abstract

The inhibition efficiency (*IE*) of an aqueous extract of *Beta vulgaris* (beetroot) in controlling corrosion of mild steel in simulated oil well water (SOWW) in the presence and absence of Zn^{2+} has been evaluated by weight loss method. The formulation consisting of 10% aqueous extract of *Beta vulgaris* extract and 50 ppm Zn^{2+} offers 94% inhibition efficiency to mild steel immersed in simulated oil well water. A synergistic effect exists between *Beta vulgaris* extract and 50 ppm Zn^{2+}.The polarization study reveals that this formulation acts as a barrier film controlling the cathodic reaction predominantly. The corrosion potential is shifted from –777 mV SCE to –789 mV SCE. The inhibitor system functions as mixed type of inhibitor because the shift in corrosion potential is within 50 mV. The linear polarization value increases from 482 Ohm·cm^2 to 1838 Ohm·cm^2. The corrosion current decreases from $1.034 \cdot 10^{-4}$ A/cm^2 to $1.887 \cdot 10^{-5}$ A/cm^2. These factors confirm that the *Beta vulgaris* extract controls the corrosion of mild steels in SOWW. The AC impedance spectra confirm that the protective coating is very stable as revealed by the fact that in the presence of *Beta vulgaris* on mild steel, its charge transfer resistance increases, impedance increases, whereas double layer capacitance decreases. The surface morphology has been analyzed by SEM. FTIR spectra study leads to the conclusion that the Fe^{2+}–betanin complex formed on the anodic sites of the metal surface controlled the anodic reaction, and $Zn(OH)_2$ formed on the cathodic sites of the metal surface controlled the cathodic reaction. Synergism parameters are found to be greater than 1 indicating that a synergistic effect exists between *Beta vulgaris* and Zn^{2+}. SEM study reveals that in presence of inhibitor system the surface of the metal becomes very smooth. The outcome of the study may be used in petroleum industry. The inhibitor formulation may be added along with mild steel pipelines carrying oil well water.

Received: November 30, 2021. Published: January 19, 2022 doi: 10.17675/2305-6894-2022-11-1-4

Keywords: *Beta vulgaris, corrosion inhibitor, simulated oil well water, polarisation study, petroleum technology, FTIR, AC impedance spectra and SEM, synergism parameter.*

Introduction

Corrosion can be considered as one of the worst technical calamities of our time. Corrosion is a predictable problem faced by almost all industries. Besides from its direct costs in dollars, corrosion is a serious problem because it definitely contributes to the depletion of our natural resources. Corrosion studies have also become important due to increasing awareness of the need to conserve the world's metal resources [1–3].

Now-a-days more attention has been paid to control the metallic corrosion, due to increasing use of metals in all fields of technology. The economic aspect combined with security and environmental concerns have provided continuous motivation for the research community to develop new methods to reduce the impact of corrosion. Material selection is one of the general approaches used to prevent corrosion. Apart from specific requirements related to the actual application and/or the corrosion environment, there are also general criteria to be considered in material selection.

Mild steel, the most widely used engineering material, accounts for approximately 85%, of the annual steel production worldwide. Despite its relatively limited corrosion resistance, mild steel is used in large tonnages in marine applications, nuclear power and fossil fuel power plants, transportation, chemical processing, petroleum production and refining, pipelines, mining, construction and metal-processing equipment.

The selection of pipe for a particular situation is dependent on what is going through the pipe, the pressure and temperature of the contents. Pipes are fabricated from different material types to suit stringent needs and services desired. The most commonly used material for petroleum pipelines is mild steel because of its strength, ductility, weldability and it is amenable to heat treatment for varying mechanical properties [4]. However, mild steel corrodes easily because all common structural metals form surface oxide films when exposed to pure air but the oxide formed on mild steel is readily broken down, and in the presence of moisture it is not repaired [5].

Corrosion inhibitor is defined as the chemical substance, which when added in small amount to the corrosive environment effectively reduces the corrosion rate when present in small amount without changing the concentration of another corrosive agent. A few organic compounds containing N, S and O hetero atoms with aromatic ring and lone pair of electrons having heterocyclic compounds are used as corrosion inhibitors and their synthesis is continuously being done [6–8].

Corrosion inhibitor adsorbs on the metal surface by blocking the active sites and hence reduces the rate of corrosion. The adsorption by heterocyclic compounds on metal surface is through the lone pair of electrons on the compounds. The heteroatom with higher electron density is required to coordinate with metal ion. The electron density on these compounds is the directly related to the percent (inhibition efficiency) *IE* of the corrosion inhibitor [9].

Most of the synthetic inhibitors (heterocyclic compounds) are not favourable as it is highly poisonous to the living organism. Therefore, most of the researches are focusing on the less toxic inhibitors derived from plant extracts. The plant extracts which show better

anticorrosive properties are less toxic and less cost. The plant extracts contain large numbers of heteroatom functionalized organic compounds, which increases the corrosion inhibition rate. Plant products are low cost, easily available and non-conventional source of materials. The extracts from their leaves, barks, seeds, fruits and roots comprise of mixture of organic compounds containing nitrogen, sulphur and oxygen atoms [10]. The list of works done on the use of plants extract as corrosion inhibitors are endless, to mention but few are extract of fenu greek seeds and leaves [11], *L. Dopa* [12], *Azardiracta Indica* [13], *Emilia Sonchifolia* and *Vitex Doniana* [14], *Adhatoda Vasica* [15], *Phyllanthus Amarus* [16] extracts. Rajendran *et al*. have extensively used extracts of plant materials as corrosion inhibitors [17–21].

In the present study, the inhibitive effect of the extract of *Beta vulgaris* on mild steel in SOWW has been investigated using the weight loss method, potentiodynamic polarization, electrochemical impedance spectroscopy technique. Characterization of the *Beta vulgaris* was carried out using FTIR spectroscopy. Meanwhile, the surface of the mild steel electrode with and without inhibitor molecules was examined using SEM and AFM spectroscopic techniques.

Experimental

Preparation of inhibitor (Beta vulgaris)

An aqueous extract of *Beta vulgaris* was prepared by grinding 10 g of *Beta vulgaris* with double distilled water, filtering the suspending impurities, and making up to 100 mL. The extract was used as corrosion inhibitor in the present study.

Preparation of specimen

The nominal composition of mild steel specimen has been given in the following Table 1.

Table 1. Composition of mild steel.

Name	Average %	Abs. Std. Dev	Ref. Std. Dev	1	2
C	0.101	0.0014	1.4	0.102	0.1
Si	0.055	0.0021	3.89	0.053	0.056
Mn	1.629	0.0057	0.35	1.633	1.625
P	0.0087	0.0003	3.25	0.0085	0.0089
S	0.0028	0.0003	10.1	0.0026	0.003
Cr	0.036	0.0014	3.93	0.037	0.035
Mo	0.0086	0.00007	0.83	0.0086	0.0085
Ni	0.033	0.0007	2.18	0.033	0.32
Cu	0.0063	0.00007	1.13	0.0062	0.0063
Al	0.044	0.0014	3.21	0.043	0.045

Name	Average %	Abs. Std. Dev	Ref. Std. Dev	1	2
As	0.0011	0	0	0.0011	0.011
B	0.0027	0.0005	18.68	<0.00010	<0.00010
Bi	<0.00010	0.00002	84.85	<0.0025	0.003
Ce	0.0032	0.0013	42.65	0.0041	0.0022
Co	0.011	0	0	0.011	0.011
Mg	0.0003	0	0	0.0003	0.0003
Nb	0.03	0.0007	2.4	0.029	0.03
Pb	0.0081	0.0013	15.71	0.0072	0.009
Sb	0.004	0.0004	8.95	0.0037	0.0042
Sn	0.0034	0	0	0.0034	0.0034
Ta	0.03	0.0071	23.57	0.025	0.035
La	0.0071	0	0	0.0071	0.0071
Ti	0.0035	0	0	0.0035	0.0035
V	0.138	0.0014	1.02	0.137	0.139
W	0.071	0.0078	11.03	0.076	0.065
Zn	0.0024	0	0	0.0024	0.0024
Zr	0.0051	0.0002	0.2	0.0052	0.0049
Se	<0.0005	0.0001	4.42	<0.0005	<0.0005
N	0.0093	0.00007	0.76	0.0092	0.0093
Ca	0.0014	0.0001	10.1	0.0013	0.0015
Te	0.0026	0.0025	97.91	<0.0010	0.0044
Fe	97.74	0	0	97.74	97.74

Specimens of dimensions $4.0 \times 1.0 \times 0.2$ cm were used for weight loss and electrochemical studies. The specimens were embedded in epoxy resin leaving a working area of 1 cm^2 for electrochemical studies. The surface preparation of the mechanically abraded specimens was carried out using different grades of silicon carbide emery paper (up to 1200 grit) and subsequent cleaning with acetone and rinsing with double-distilled water were done before each experiment.

Preparation of simulated oil well water (SOWW)

In 100 mL of double distilled water, sodium chloride (3.5 g), calcium chloride (0.305 g) and magnesium chloride (0.186 g) are added. Just before experiment, add 0.067 g sodium sulfide

and 0.4 mL of concentrated hydrochloric acid to generate hydrogen sulfide gas to form a simulated oil well water containing 100 ppm of H_2S.

Weight loss method

Mild steel specimens in triplicate were immersed in 100 mL of the simulated oil well water containing various concentrations of the inhibitor (aqueous extract of *Beta vulgaris*) in the presence and absence of Zn^{2+} for one day. The weight of the specimens before and after immersion was determined using a Shimadzu balance, model AY60. The corrosion products were cleaned with Clarke's solution [22]. The difference between initial weight prior to deployment and final weight was used for calculation of corrosion rate by using the following formula [23]:

$$\text{Corrosion rate} = \frac{W}{A \cdot T} \tag{1}$$

where, corrosion rate is expressed in terms of metal loss (mg) per square decimeter area per day (mdd), W is loss in weight (mg), A is area of panels (dm^2) and T is exposure time (days).

The inhibition efficiency was calculated using the relation:

$$\text{Inhibition efficiency}\left(\%IE\right) = \frac{CR_1 - CR_2}{CR_1} \cdot 100 \tag{2}$$

where, CR_1 = corrosion rate in the absence of inhibitor, CR_2 = corrosion rate in the presence of inhibitor.

Potentiodynamic polarization studies

The corrosion resistance of mild steel has been measured by electrochemical studies such as polarisation study. A CHI electrochemical work station with impedance model 660A was used for this purpose. A three electrode cell assembly (Figure 1) was used in the present study.

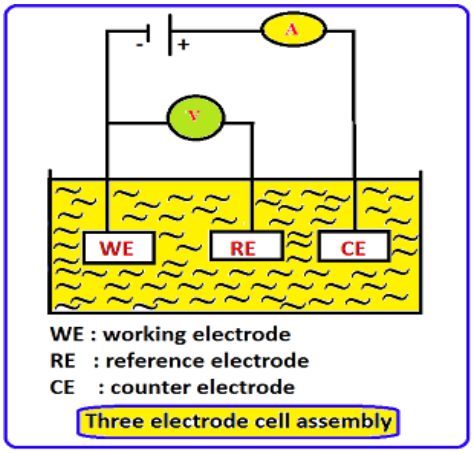

Figure 1. Three electrode cell assembly.

Mild steel was used as working electrode; saturated calomel electrode was used as reference electrode and platinum electrode was used as counter electrode. From the polarisation study corrosion parameters such as corrosion potential (E_{corr}), corrosion current (I_{corr}) and Tafel slope values (anodic = b_a and cathodic = b_c) and linear polarization resistance (*LPR*) values were calculated.

AC impedance spectra

The instrument used for polarization was used for AC impedance study also. The cell set-up was the same as that had been used for polarization measurements. The real part and imaginary part of the cell impedance were measured in Ohms at various frequencies. From Nyquist plot the values of charge transfer resistance (R_{ct}) and the double layer capacitance, (C_{dl}), were calculated.

Surface examination study

The mild steel specimens were immersed in various test solutions for a period of one day. After one day the specimens were taken out and dried. The nature of the film formed on the surface of metal specimens was analyzed by surface analysis technique, FTIR spectra, AFM and SEM.

Fourier Transform Infrared (FTIR) Spectroscopy

The functional groups present in *Beta vulgaris* and the film formed on the metal surface were determined using the Perkin-Elmer 1600 Fourier transform infra-red spectrophotometer. The analysis was carried out by scanning the sample through a wave number range of 400 to 4000 cm^{-1}.

Scanning Electron Microscopy (SEM):

The mild steel specimens immersed in various test solutions for one day were taken out, rinsed with double distilled water, dried and subjected to the surface examination. The surface morphology measurements of the mild steel surface were carried out by scanning electron microscopy (SEM) using JEOL MODEL6390 computer-controlled scanning electron microscope.

Atomic Force Microscopy (AFM)

Atomic Force Microscope (AFM) is a new technique which allows metal surface to be imaged at higher resolutions and accuracies than ever before. The mild steel specimens were immersed in SOWW (blank) and in the inhibitor system for one day. The mild steel specimens were removed, rinsed with double distilled water, dried, and subjected to the surface examination. Veeco Innova model was used to observe the mild steel surface in tapping mode, using cantilever with linear tips. The scanning area in the images was

50×50 μm and the scan rate was 0.6 $Hz \cdot s^{-1}$. A two dimensional, and a three dimensional topography of metal surface films gave various roughness parameters of the film.

Results and Discussion

Analysis of results of weight loss method

Inhibition efficiencies (*IE*%) of *Beta vulgaris* – Zn^{2+} systems in controlling corrosion of mild steel (whose composition is given in Table 1) immersed in aqueous SOWW in the presence and absence of inhibitor system are given in Table 2. It is obvious that *Beta vulgaris* alone has poor inhibition efficiency. In the presence of 50 ppm concentration of Zn^{2+} the *IE* of *Beta vulgaris* becomes effective. A synergistic effect exists between *Beta vulgaris* and Zn^{2+}. For example, 10 mL of *Beta vulgaris* has only 59% *IE* and 50 ppm of Zn^{2+} has 12% *IE*. However, their combination of 10 mL of *Beta vulgaris* with 50 ppm of Zn^{2+} has 94% *IE*. This denotes that a synergistic effect exists between *Beta vulgaris* and Zn^{2+} [24] shown in Table 3. Synergism parameter is calculated to evaluate the synergistic effect existing between inhibitors. Synergistic effects have been calculated considering the blocking effect. The synergism parameter (S_I) can be calculated using the relationship:

$$S_I = \frac{1-\theta_{1+2}}{1-\theta'_{1+2}} \tag{3}$$

$$\theta_{1+2} = (\theta_1 + \theta_2) - (\theta_1 \cdot \theta_2) \tag{4}$$

Where θ_1 is surface coverage of inhibitor (*Beta vulgaris*), θ_2 is surface coverage of inhibitor (Zn^{2+}), θ'_{1+2} is combined surface coverage of inhibitors (*Beta vulgaris*) and (Zn^{2+}).

Surface coverage assuming the blocking effect:

$$\text{Surface coverage} = \frac{IE\%}{100}$$

Table 2. Gravimetric data of mild steel in SOWW with and without inhibitor – Zn^{2+} system at 303 K.

Extract (%)	Zn^{2+} 0 ppm		Zn^{2+} 50 ppm	
	***CR* (mdd)**	***IE* (%)**	***CR* (mdd)**	***IE* (%)**
0	58.18	–	51.19	12
2	33.16	43	10.47	82
4	30.83	47	8.72	85
6	28.50	51	6.98	88
8	26.18	55	5.23	91
10	23.85	59	3.49	94

Synergistic effect means that, a mixture of inhibitors shows better inhibition efficiency than the individual members. The synergism parameters (S_I) have been calculated from the inhibition efficiencies and the surface coverage, assuming the blocking effect [25]. The synergism parameters are found to be greater than 1, indicating that a synergistic effect exists between *Beta vulgaris* and Zn^{2+}.

Table 3. Synergism parameters for *Beta vulgaris* extract – Zn^{2+}(50 ppm) system.

***Beta vulgaris* extract (%)**	**θ_1**	**θ_2**	**θ'_{1+2}**	**S_I**
2	0.43	0.12	0.82	2.7888
4	0.47	0.12	0.85	3.1093
6	0.51	0.12	0.88	3.5933
8	0.55	0.12	0.91	4.4
10	0.59	0.12	0.94	6.013

Analysis of potentiodynamic polarisation curves

Electrochemical studies such as polarization technique has been used to confirm the formation of protective film formed on the metal surface during corrosion inhibition process. If a protective film forms on the metal surface, the linear polarization resistance value (*LPR*) increases and corrosion current value (I_{corr}) decreases [26–28].

The potentiodynamic polarization curves of mild steel immersed in SOWW in the absence and presence of inhibitor system (*Beta vulgaris*+Zn^{2+}) are shown in Figure 2. The corrosion parameters are given in Table 4.

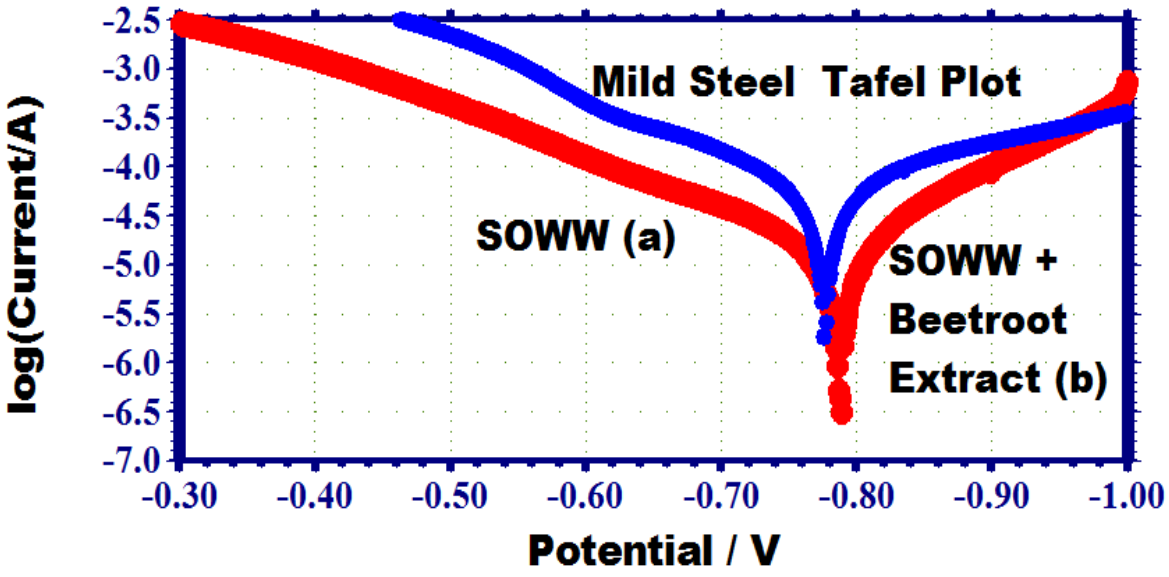

Figure 2. Polarization curves of mild steel immersed in various test solution: a) SOWW; b) SOWW + *Beta vulgaris* extract 10% + Zn^{2+} 50 ppm.

Table 4. Corrosion parameters of mild steel immersed in SOWW in the absence and presence of *Beta vulgaris* extract and 50 ppm of Zn^{2+} obtained by polarization study.

System	E_{corr} mV *vs.* SCE	b_c mV/decade	b_a mV/decade	*LPR* Ohm·cm^2	I_{corr} A/cm^2
SOWW	–777	265	202	482	$1.034 \cdot 10^{-4}$
SOWW + *Beta vulgaris* extract	–789	132	202	1838	$1.887 \cdot 10^{-5}$

When mild steel was immersed in aqueous SOWW the corrosion potential was –777 V *vs.* SCE. When *Beta vulgaris* (10 mL) and Zn^{2+} (50 ppm) were added to the above system the corrosion potential shifted to –789 V *vs.* SCE. This indicates that the inhibitory composition acts as mixed-type inhibitor. Further the *LPR* values increases from 482 Ohm·cm^2 to 1838 Ohm·cm^2. The corrosion current decreases from $1.034 \cdot 10^{-4}$ A/cm^2 to $1.887 \cdot 10^{-5}$ A/cm^2. Thus the Polarization study confirms the formation of protective film on the metal surface.

Analysis of AC impedance spectra

AC impedance spectra (electrochemical impedance spectra) have been used to confirm the formation of protective film on the metal surface. If a protective film is formed on the metal surface, charge transfer resistance (R_{ct}) increases. Charge transfer resistance control the process of electron transfer from one phase (*e.g.*, electrode) to another (*e.g.*, liquid). Double layer capacitance value (C_{dl}) decreases and impedance log(Z/Ohm) value increases [29]. Double layer capacitance is the storing of electrical energy by means of the electrical double layer effect. This electrical phenomenon appears at the interface between a conductive electrode and an adjacent liquid electrolyte as observed, for example, in a super capacitor.

The AC impedance spectra of mild steel immersed in simulated oil well water in the absence and presence of inhibitors (*Beta vulgaris* – Zn^{2+}) are shown in Figure 3 (Nyquist plots).

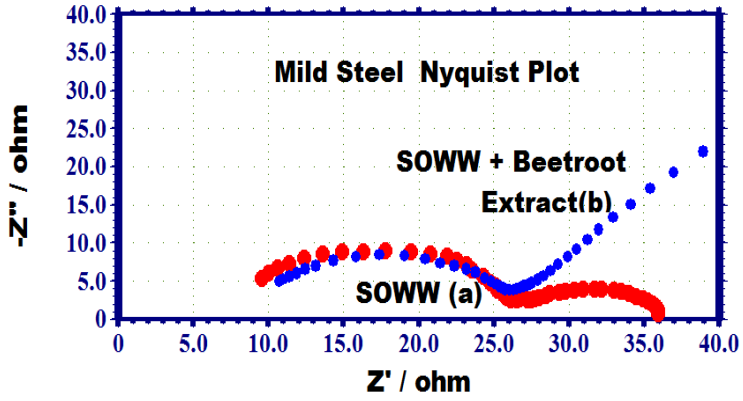

Figure 3. AC impedance curves of mild steel immersed in various test solutions (Nyquist plots): a) SOWW; b) SOWW + *Beta vulgaris* extract 10% + Zn^{2+} 50 ppm.

It is observed from Figure 3 that when mild steel is immersed in aqueous SOWW, two semicircles are observed. This is characteristic of a protective film formed and then broken. The breaking of the film is due to the presence of corrosive ions in solution. The equivalent circuit diagram for such a system is shown in Figure 4.

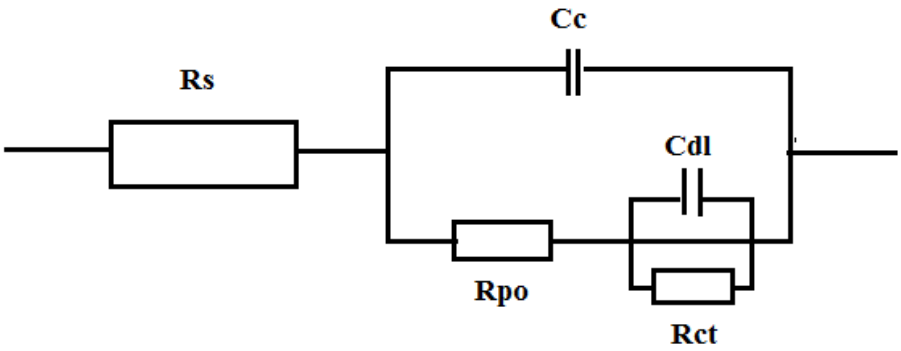

Figure 4. Equivalent circuit for a failed coating. C_c – the capacitance of the intact coating, R_{po} – pore resistance, R_{ct} – charge transfer resistance, R_s – solution resistance, C_{dl} – double layer capacitance.

The AC impedance spectra of mild steel immersed in aqueous SOWW in the presence and absence of inhibitors (*Beta vulgaris* – Zn^{2+}) are shown in Figure 5 and Figure 6 (Bode plots). The AC impedance parameters namely charge transfer resistance (R_{ct}) and double layer capacitance value (C_{dl}) derived from Nyquist plots and the impedance log(Z/Ohm) values derived from Bode plots respectively are given in Table 5.

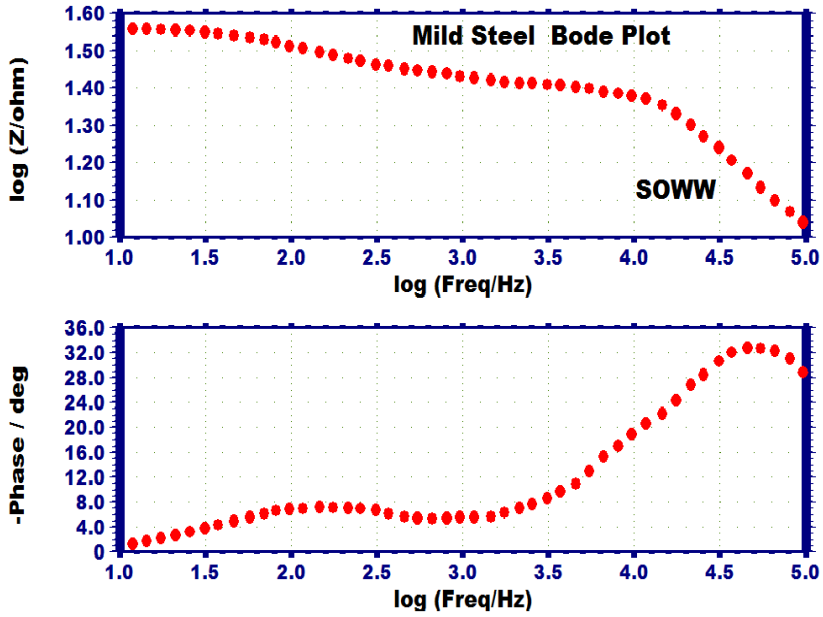

Figure 5. AC impedance spectra of mild steel immersed in SOWW (Bode plots).

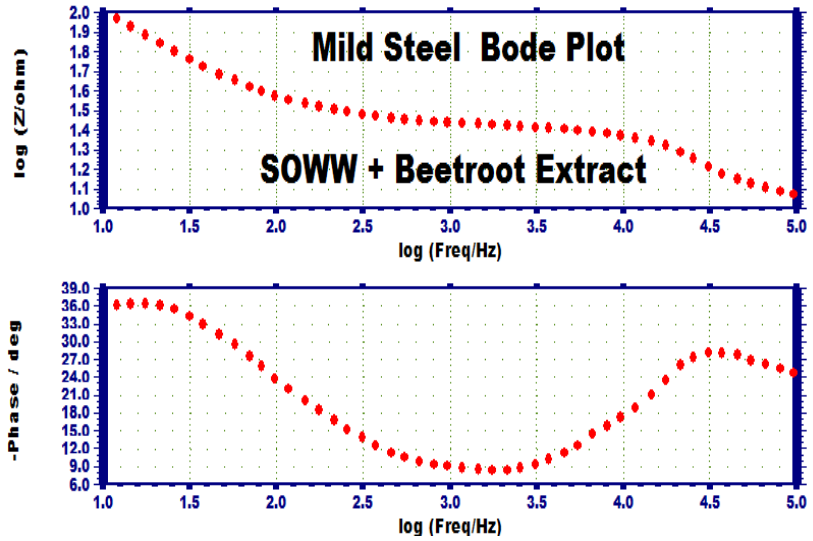

Figure 6. AC impedance spectra of mild steel immersed in SOWW+10% *Beta vulgaris*+50 pm of Zn^{2+} system (Bode plots).

Table 5. Corrosion parameters of mild steel immersed in SOWW in the absence and presence of *Beta vulgaris* extract and 50 ppm of Zn^{2+} obtained by AC impedance spectroscopy.

System	R_{ct} Ohm·cm^2	C_{dl} F/cm^2	Impedance log(*Z*/Ohm)
SOWW	27.871	$1.82 \cdot 10^{-7}$	1.577
Beta vulgaris	67.385	$7.56 \cdot 10^{-8}$	1.999

It is observed that when the inhibitors (*Beta vulgaris* (10%)+Zn^{2+} (50 ppm)) are added to SOWW, the charge transfer resistance increases from 27.871 Ohm·cm^2 to 67.385 Ohm·cm^2. The C_{dl} value decreases from $1.82 \cdot 10^{-7}$ F/cm^2 to $7.56 \cdot 10^{-8}$ F/cm^2. The impedance value [log(*Z*/Ohm)] increases from 1.577 to 1.999. These observations lead to the conclusion that a protective film is formed on the metal surface [30, 31] in the presence of inhibitors (*Beta vulgaris* – Zn^{2+}). Equivalent circuit diagram for such a system is shown in Figure 7. The circuit models a cell where polarization is due to a combination of kinetic and diffusion process.

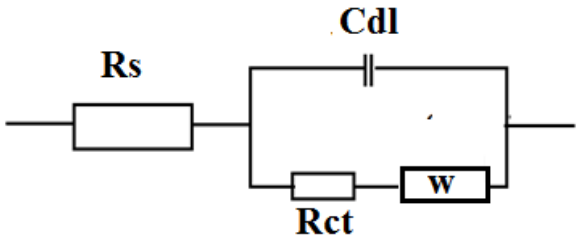

Figure 7. Equivalent circuit diagram for a diffusion controlled process. R_s – solution resistance, R_{ct} – charge transfer resistance, W – Warburg diffusion resistance, C_{dl} – double layer capacitance.

Analysis of FTIR spectra

FTIR spectra have been used to analyze the protective film formed on the metal surface [32–34]. The active principle in an aqueous extract of *Beta vulgaris* is betanin. The red colour of the extract is due to betanin [35]. The structure of pure betanin is shown in Figure 8.

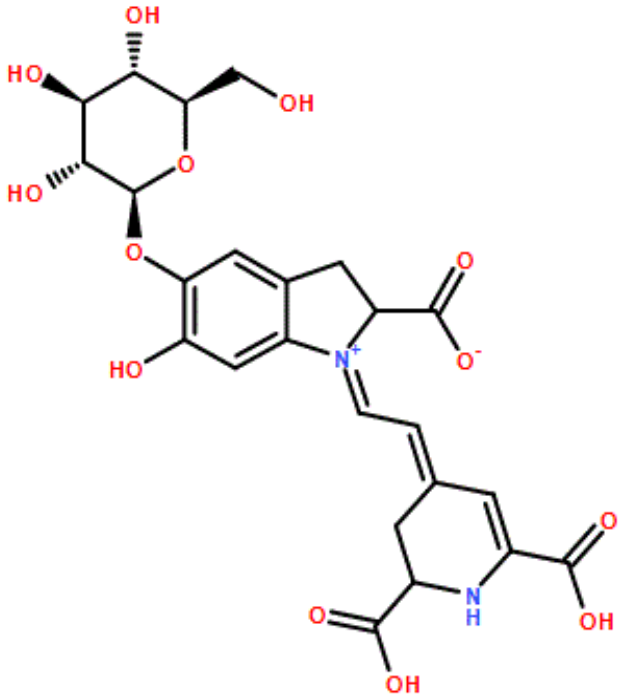

Figure 8. Structure of betanin (root of *Beta Vulgaris*).

A few drops of an aqueous extract of *Beta vulgaris* were dried on a glass plate. A solid mass was obtained. Its FTIR spectrum is shown Figure 9. The C=O stretching frequency appears at 1632 cm^{-1}. The C–H stretching frequency appears at 2969 cm^{-1}, 2921 cm^{-1}. The C–O–C stretching frequency appears at 1268 cm^{-1}. The OH stretching frequency appears at 3434 cm^{-1}. Thus the structure of betanin is confirmed by FTIR spectra [36]. The FTIR spectrum of the film formed on the surface of the metal after immersion in the solution containing simulated oil well water, 10% of *Beta vulgaris* and 50 ppm of Zn^{2+} is shown in Figure 10. The C=O stretching frequency shifts from 1632 cm^{-1} to 1629 cm^{-1}. The OH stretching frequency shifts from 3434 cm^{-1} to 3401 cm^{-1}. The C–H stretching frequency shifts from 2969 cm^{-1} to 2921 cm^{-1}. The C–O–C stretching frequency disappeared. These shifts confirm the formation of a Fe^{2+}–betanin complex on the anodic sites of the metal surface. The peak at 690 cm^{-1} is due to metal oxygen bond. The peak at 1383 cm^{-1} is due to $Zn(OH)_2$ formed on the cathodic sites of the metal surface [37].

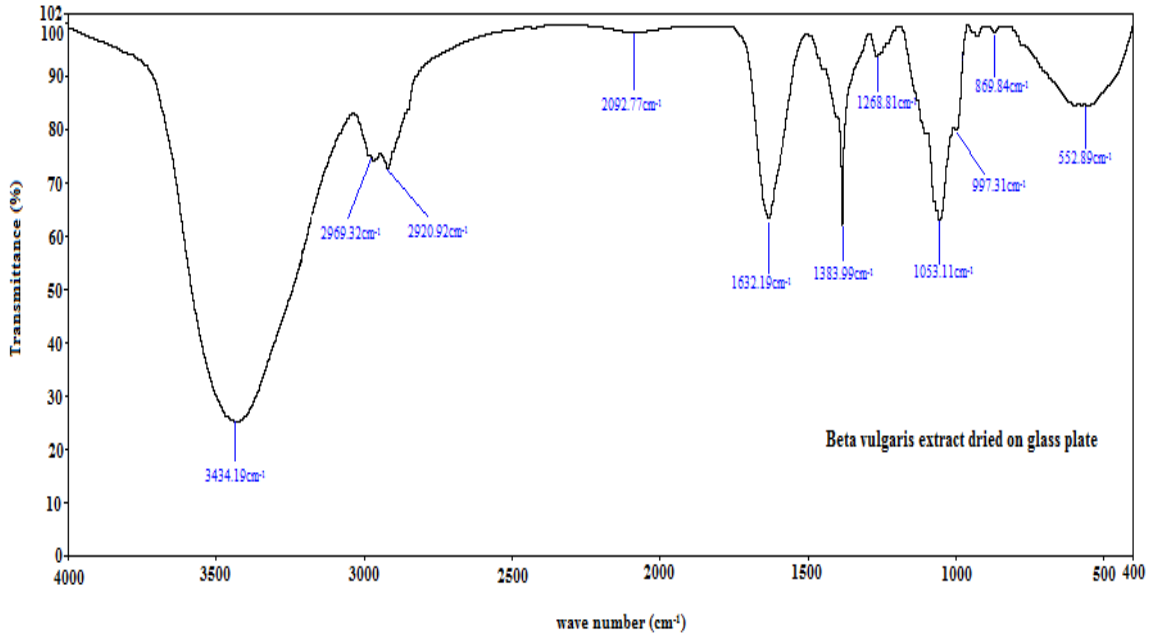

Figure 9. FTIR spectrum of pure *Beta vulgaris*.

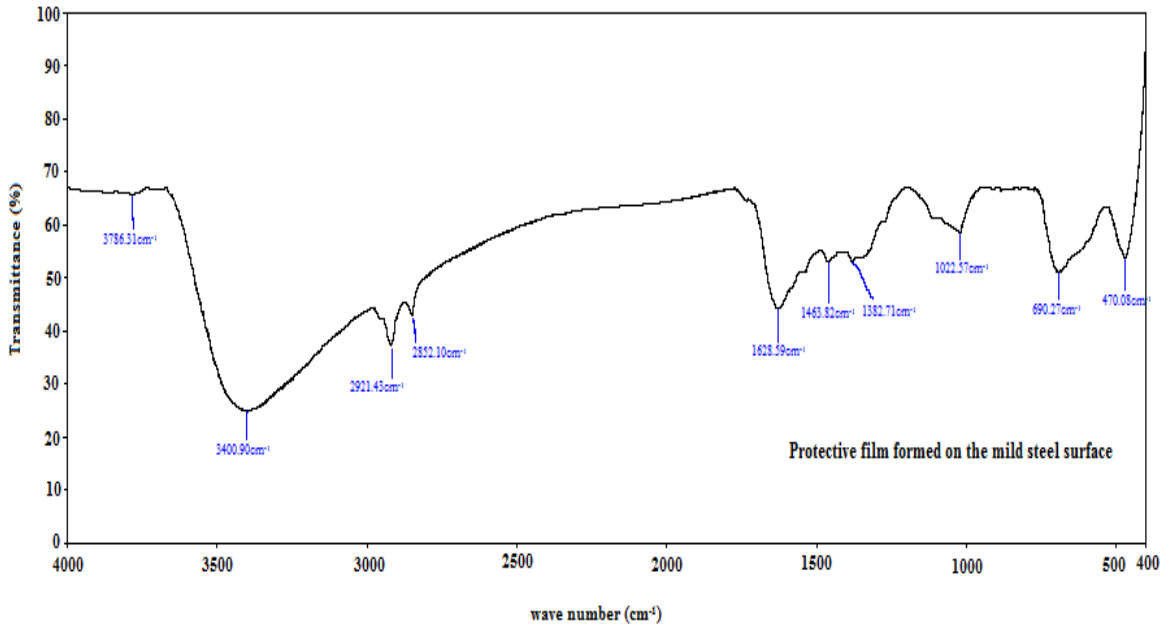

Figure 10. FTIR spectrum of a protective film formed on the mild steel after immersion in SOWW containing 10% of *Beta vulgaris* and 50 ppm of Zn^{2+}.

Analysis of Atomic Force Microscopy characterization

Atomic Force Microscopy (AFM) is an effective method for investigation and collection of roughness statistics from a variety of surfaces. AFM image analysis was performed to obtain the average roughness, R_a (the average deviation of all points roughness profile from a mean line over the evaluation length), root-mean-square roughness, R_q (the average of the measured height deviations taken within the evaluation length and measured from the mean

line) and the maximum peak-to-valley ($P–V$) height values (largest single peak-to-valley height in five adjoining sampling heights). R_q is much more sensitive than R_a to large and small height deviations from the mean [38].

The two dimensional (2D), three dimensional (3D) AFM morphologies and the AFM cross-sectional profile for polished mild steel surface, mild steel surface immersed in aqueous SOWW (blank) and mild steel surface immersed in aqueous SOWW with *Beta vulgaris* – Zn^{2+} (50 ppm) are shown in Figures 11 and 12 respectively. The different parameters R_q, R_a, and $P–V$ values from the AFM images of metal surfaces are given in Table 6 for the polished mild steel, mild steel surface immersed in aqueous SOWW and mild steel surface immersed in aqueous SOWW with *Beta vulgaris* – Zn^{2+} (50 ppm).

Table 6. AFM parameters for mild steel surface immersed in inhibited and uninhibited environment.

Samples	Average Roughness (R_a) (nm)	RMS Roughness (R_q) (nm)	Maximum peak – valley height (R_y) (nm)
Polished	4.8228	6.3498	37.465
SOWW	288.73	382.33	1849.3
SOWW + *Beta vulgaris* + Zn^{2+}	26.713	36.905	199.53

In Figures 11a and 12a the surface topography of un corroded metal surface is shown. The values of R_q, R_a and $P–V$ height for the polished mild steel surface are 6.3498 nm, 4.8228 nm and 37.465 nm, respectively. The data indicate a homogeneous surface. The slight roughness formed on the polished mild steel surface is due to atmospheric corrosion.

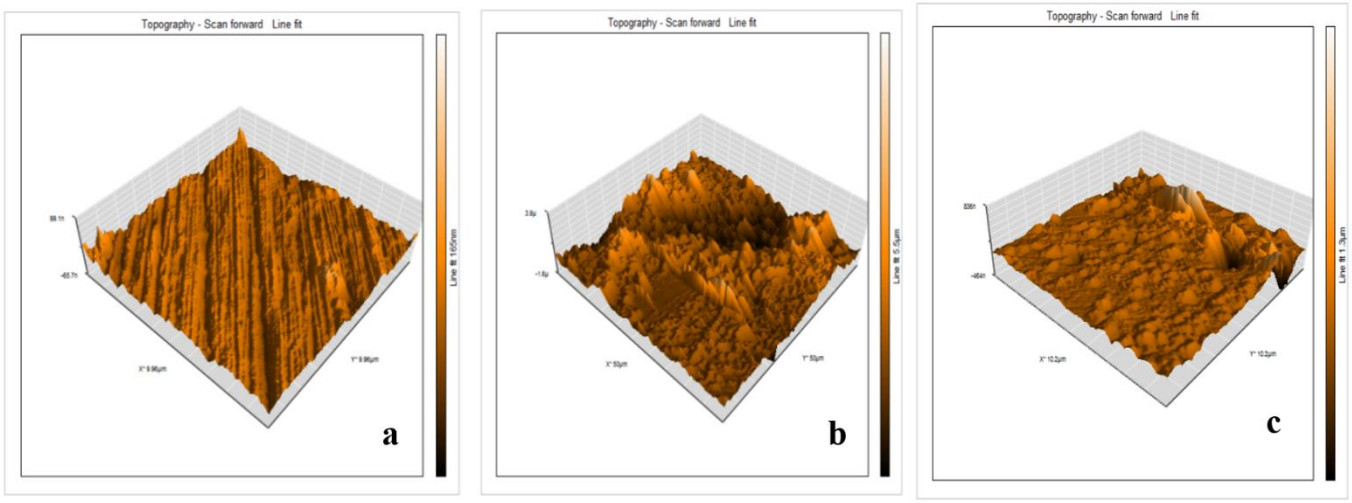

Figure 11. Three dimensional AFM images of the surface of: a) as polished mild steel (control); b) mild steel immersed in SOWW (blank); c) mild steel immersed in SOWW containing *Beta vulgaris* (10%) + Zn^{2+} (50 ppm).

Figures 11b and 12b show the pitted, corroded metal surface in the absence of the inhibitor, immersed in aqueous SOWW. The R_q, R_a and $P–V$ height values for the mild steel surface immersed in aqueous SOWW are 382.33 nm, 288.73 nm and 1849.3 nm respectively. These data indicate that mild steel surface immersed in aqueous SOWW has severe surface roughness than the polished metal surface, which shows that the unprotected mild steel surface is too rough due to the corrosion of the steel in aqueous SOWW environment.

Figures 11c and 12c show the complete changes on the mild steel surface after immersion in aqueous SOWW containing *Beta vulgaris* – Zn^{2+} (50 ppm). The R_q, R_a and $P–V$ height values for the mild steel surface immersed in the above experimental solution are 36.905 nm, 26.713 nm and 199.53 nm respectively. The R_q, R_a and $P–V$ height values are considerably less in the inhibited environment compared to the uninhibited environment. So, these parameters confirm that the surface is smoother than the uninhibited environment. The smoothness of the surface is due to the formation of a compact protective film of Fe^{2+} – *Beta vulgaris* complex and $Zn(OH)_2$ on the metal surface, thereby inhibiting the corrosion of mild steel [39, 40].

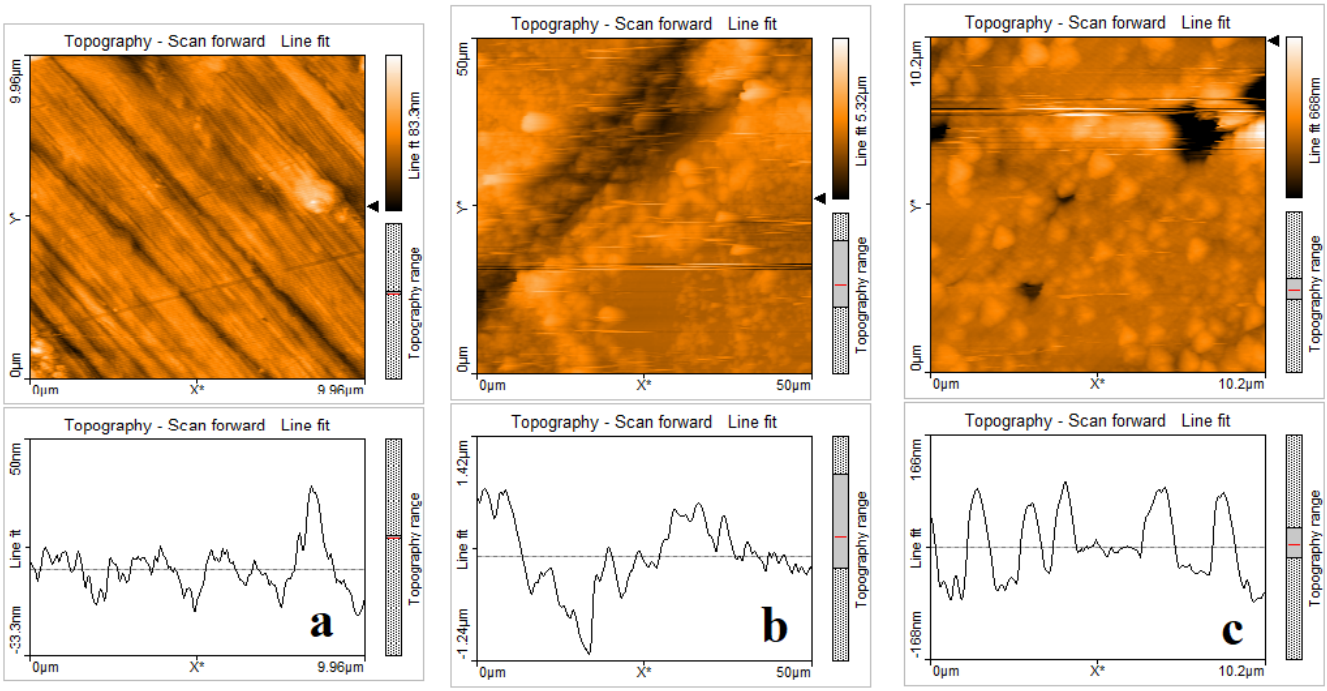

Figure 12. AFM cross-sectional images of the surface of: a) as polished mild steel (control); b) mild steel immersed in SOWW (blank); c) mild steel immersed in SOWW containing *Beta vulgaris* (10%) + Zn^{2+} (50 ppm).

The R_q, R_a and $P–V$ values of mild steel immersed in the aqueous SOWW in the presence of inhibitors, are greater than the R_q, R_a and $P–V$ values of polished metal surface. This confirms the presence of the film on the metal surface, which is protective in nature.

Analysis of Scanning Electron Microscope (SEM) images

SEM provides a pictorial representation of the surface. SEM micrographs [41, 42] are used to examine the nature of the surface film formed on the metal in the presence and absence of inhibitors. The SEM images of mild steel and mild steel immersed in aqueous SOWW in the presence and absence of inhibitor system are shown in Figure 13 as images (a, b and c) respectively. In Figure 13(a) the image arrived by the SEM micrographs of polished mild steel surface illustrates the smooth surface of the metal and the absence of any corrosion products which could form on the metal surface. The image shown in Figure 13(b) denotes the effect of SEM micrograph of mild steel immersed in aqueous SOWW and verifies that the surface is corroded in an inhibitor free solution. The presence of *Beta vulgaris* – Zn^{2+} (50 ppm) mixture in aqueous SOWW, suppresses the rate of corrosion which results in the formation of insoluble complex on the surface of the metal (Zn^{2+}+*Beta vulgaris* complex). The surface appears to be smooth [Figure 13(c)].

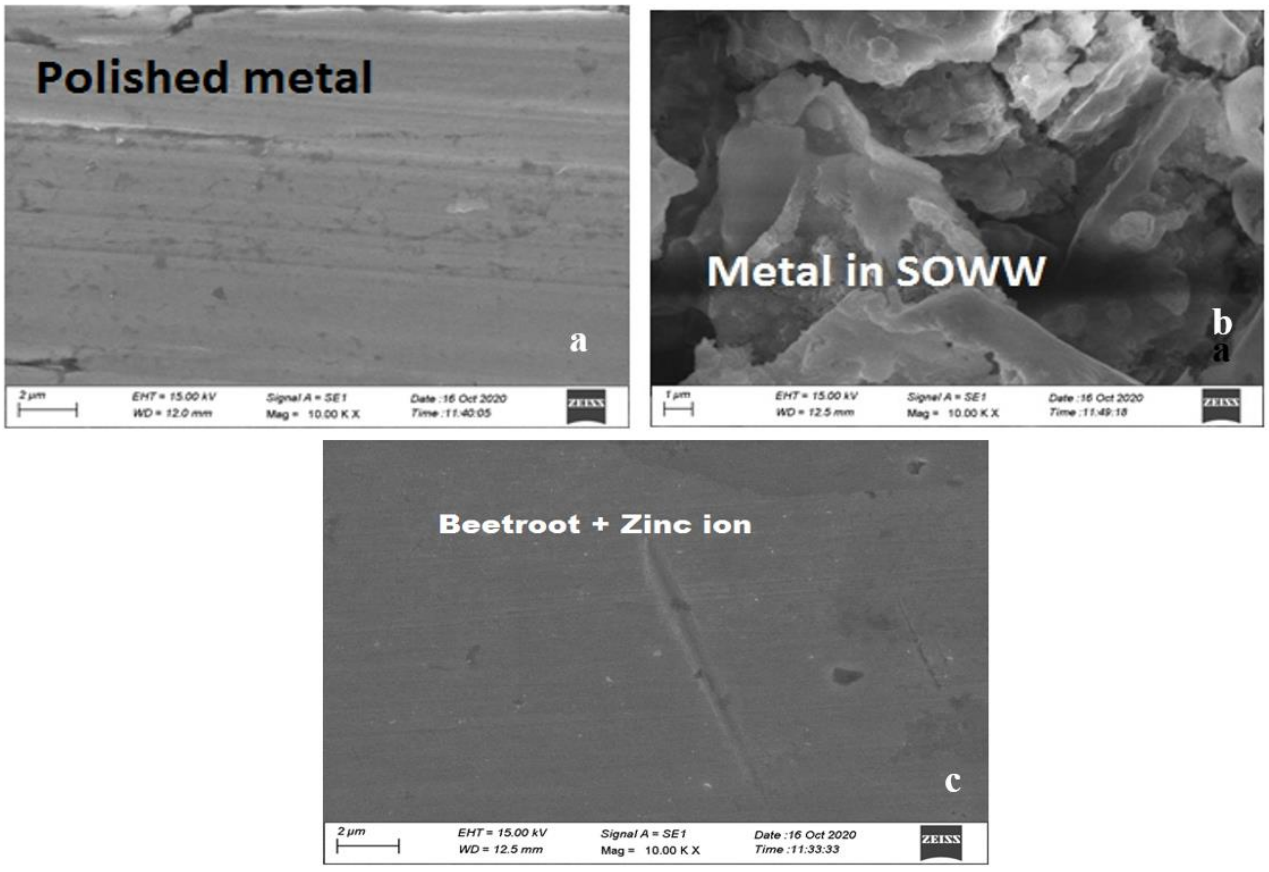

Figure 13. SEM micrographs of (a) polished metal; (b) mild steel immersed in aqueous SOWW; (c) mild steel immersed in aqueous SOWW containing *Beta vulgaris* (10%)+Zn^{2+} (50 ppm).

Conclusion

- Mild steel can be used in petroleum industry to carry oil well water. When mild steel comes in contact with the environment, especially oxygen and moisture, they deteriorate. This process, we call corrosion.
- To mitigate this corrosion problem an extracts of *Beta vulgaris* was used.
- The corrosion protection nature of *Beta vulgaris* extract with 50 ppm of Zn^{2+} has been evaluated by weight loss method which reveals that the extract of *Beta vulgaris* offers 94% inhibition efficiency to mild steel immersed in simulated oil well water.
- Polarization study reveals that *Beta vulgaris* extract and Zn^{2+} (50 ppm) system functions as mixed type of inhibitor.
- The corrosion potential is shifted from –0.777 V SCE to –0.789 V SCE. The linear polarization resistance value increases from 482 $Ohm \cdot cm^2$ to 1838 $Ohm \cdot cm^2$. The corrosion current decreases from $1.034 \cdot 10^{-4}$ A/cm^2 to $1.887 \cdot 10^{-5}$ A/cm^2. These facts confirm that the extract of *Beta vulgaris* controls the corrosion of mild steel in SOWW.
- The AC impedance spectra confirm that the protective film is very stable as revealed by the fact that in the presence of inhibitor on mild steel, its charge transfer resistance increases and impedance increases, whereas corrosion current decreases to a great extent.
- FTIR study reveals that a protective film consisting of Fe^{2+} – betanin complex and $Zn(OH)_2$ is formed on the metal surface.
- SEM images of various metal surfaces reveal that in the presence of SOWW alone, pits are noticed on mild steel whereas in the presence of *Beta vulgaris* – Zn^{2+} (50 ppm) the surface appears to be smooth, when immersed in SOWW.
- Furthermore, atomic force microscopic study has indicated the presence of smooth surface in case of inhibited mild steel when compared to the uninhibited sample.
- Synergism parameters are found to be greater than 1 indicating that a synergistic effect exists between *Beta vulgaris* and Zn^{2+}.

Reference

1. M.A. Abdel-Gaber, E. Khamis, S. Habo-Eidahab and Mh. Adeel, Inhibition of aluminium corrosion in alkaline solutions using natural compound, *Mater. Chem. Phys.*, 2008, **109**, no. 2–3, 297–305. doi: 10.1016/J.MATCHEMPHYS.2007.11.038
2. E.I. Ating, S.A. Umoren, I.I. Udousoro, E.E. Ebenso and A.P. Udoh, Leaves extract of *Ananas sativum* as green corrosion inhibitor for aluminium in hydrochloric acid solutions, *Green Chem. Lett. Rev.*, 2010, **3**, 61–68. doi: 10.1080/17518250903505253
3. W.A. Badaway, F.M. AlKharafi and A.S. El-Azab, Electrochemical behaviour and corrosion inhibition of Al, Al-6061 and Al–Cu in neutral aqueous solutions, *Corros. Sci.*, 1999, **41,** no. 4, 709–727. doi: 10.1016/S0010-938X(98)00145-0
4. W.F. Smith and J. Hashemi, *Foundations of Material Science and Engineering*, Fourth Edition, McGraw-Hill, New York, 2006.

5. A.Y. Badmos and H.A. Ajimotokan, *The Corrosion of Mild Steel in Orange Juice Environment*, Technical Report No: 2009-02, Department of Mechanical Engineering, University of Ilorin, Nigeria, 2009.
6. A.A. Al-Amiery, M.H.O. Ahmed, T.A. Abdullah, T.S. Gaaz and A.A.H. Kadhum, Electrochemical studies of novel corrosion inhibitor for mild steel in 1 M hydrochloric acid, *Results Phys*., 2018, **9**, 978–981. doi: 10.1016/j.rinp.2018.04.004
7. M. Corrales-Luna, T.L. Manh, M. Romero-Romo, M. Palomar-Pardavé and E.M. Arce-Estrada, 1-Ethyl 3-methylimidazolium thiocyanate ionic liquid as corrosion inhibitor of API 5L X52 steel in H_2SO_4 and HCl media, *Corros. Sci*., 2019, **153**, 85–99. doi: 10.1016/j.corsci.2019.03.041
8. A. Ghames, T. Douadi, S. Issaadi, L. Sibous, K.I. Alaoui, M. Taleb and S. Chafaa, Theoretical and Experimental Studies of Adsorption Characteristics of Newly Synthesized Schiff Bases and their Evaluation as Corrosion Inhibitors for Mild Steel in 1 M HCl, *Int. J. Electrochem. Sci*., 2017, **12**, 4867–4897. doi: 10.20964/2017.06.92
9. I. Ahamad, R. Prasad and M.A. Quraishi, Thermodynamic, electrochemical and quantum chemical investigation of some Schiff bases as corrosion inhibitors for mild steel in hydrochloric acid solutions, *Corros. Sci*., 2010, **52**, no. 3, 933–942. doi: 10.1016/j.corsci.2009.11.016
10. P. Arockiasamy, X.Q.R. Sheela, G. Thenmozhi, M. Franco, J.W. Sahayaraj and R.J. Santhi, Evaluation of corrosion inhibition of mild steel in 1M Hydrochloric solution by Mollugo cerviana, *Int. J. Corros*., **2014**, 2014. doi: 10.1155/2014/679192
11. A.N. Ehteram, Comparative study on the corrosion inhibition of mild steel by aqueous extract of fenugreek seeds and leaves in acidic solutions, *J. Eng. Appl. Sci*, 2008, **3**, no. 1, 23–30.
12. H.P. Sachin, M.H. Moinuddinkhan, S. Raghavendra and N.S. Bhujangaiah, L-dopa as corrosion inhibitor for mild steel in mineral acid, *Open Electrochem. J*., 2009, **1**, 15–18.
13. P.C. Okafor, E.E. Ebenso and U.J. Ekpe, Azadirachta Indica extract as corrosion inhibitor for mild steel in acidic medium, *Int. J. Electrochem. Sci*., 2010, **5**, no. 7, 978–993.
14. I.M. Iloamaeke, T.U. Onuegbu, U.C. Umeobika and N.L. Umedum, Green Approach to Corrosion Inhibition of Mild Steel Using Emilia Sonchifolia and Vitex Doniana In 2.5M HCl Medium, *Int. J. Sci. Modern Engg*., 2013, **1**, no. 3, 48–52.
15. M.R. Singh, A green Approach: A corrosion inhibition of mild steel by adhatoda vasica plant extract in 0.5 M H_2SO_4, *J. Mater. Environ. Sci*., 2013, **4**, no. 1, 119–126.
16. P.C. Okafor, M.E. Ikpi, I.E. Uwaha, E.E. Ebenso, U.J. Ekpe and S.A. Umoren, Inhibitory action of *Phyllanthus amarus* extracts on the corrosion of mild steel in acidic media, *Corros. Sci*., 2008, **50**, no. 8, 2310–2317. doi: 10.1016/j.corsci.2008.05.009
17. A. Nithya, P. Shanthy, N. Vijaya, R.J. Rathish, S.S. Prabha, R.M. Joany and S. Rajendran, Inhibition of Corrosion Of Aluminium By An Aqueous Extract Of Beetroot (Betanin), *Int. J. Nano Corr. Sci. Engg*., 2015, **2**, no. 1, 1–11.

18. N. Kavitha and P. Manjula, Corrosion Inhibition of Water Hyacinth Leaves, Zn^{2+} and TSC on Mild Steel in neutral aqueous medium, *Int. J. Nano. Corr. Sci. Engg*., 2014, **1**, no. 1, 31–38.
19. M. Sangeetha, S. Rajendran, J.S. Bama, A. Krishnaveni, P. Santhy, N. Manimaran and B. Shyamaladevi, Corrosion inhibition by an Aqueous extract of *Phyllanthus Amarus*, *Port. Electrochim. Acta*, 2011, **29**, no. 6, 429–444. doi: 10.4152/pea.201106429
20. K. Rajam, S. Rajendran and N.N. Banu, Effect of Caffeine-Zn^{2+} System in Preventing Corrosion of Carbon Steel in Well Water, *J. Chem*., 2013, **13**, 1–11. doi: 10.1155/2013/521951
21. N. Anthony, E. Malarvizhi, P. Maheshwari, S. Rajendran and N. Palaniswamy, Corrosion inhibition by caffeine Mn^{2+} system, *Indian J. Chem. Technol*., 2004, **11**, 346–350.
22. G. Wranglen, *Introduction to Corrosion and Protection of Metals*, London: Chapman and Hall, 1986, 236.
23. K. Kavitha, H.B. Sherine and S. Rajendran, Anti-corrosive properties of an aqueous extract of Chrysanthemum indicum flower, *Int. J. Corros. Scale Inhib*., 2021, **10**, no. 2, 783–800. doi: 10.17675/2305-6894-2021-10-2-19
24. J.A. Selvi, S. Rajendran, V.G. Sri, A.J. Amalraj and B. Narayanasamy, Corrosion Inhibition by Beet Root Extract, *Port. Electrochim. Acta*, 2009, **27**, no. 1, 1–11. doi: 10.4152/pea.200901001
25. P. Shanthy, J.A. Thangakani, S. Karthika, S.C. Joycee, S. Rajendran and J. Jeyasundari Corrosion inhibition by an aqueous extract of *Ervatamia divaricata*, *Int. J. Corros. Scale Inhib*., 2021, **10**, no. 1, 331–348, doi: 10.17675/2305-6894-2021-10-1-19
26. C.O. Akalezi, C.E. Ogukwe, E.A. Ejele and E.E. Oguzie, Mild steel protection in acidic media using *Mucuna pruriens* seed extract, *Int. J. Corros. Scale Inhib*., 2016, **5**, no. 2, 132–146. doi: 10.17675/2305-6894-2016-5-2-3
27. T.A. Onat, D. Yigit, H. Nazır, M. Güllü and G. Donmez, Biocorrosion inhibition effect of 2-aminopyrimidine derivatives on SRB, *Int. J. Corros. Scale Inhib*., 2016, **5**, no. 3, 273–281. doi: 10.17675/2305-6894-2016-5-3-7
28. A.S. Fouda, M.A. El-Morsy, A.A. El-Barbary and L.E. Lamloum, Study on corrosion inhibition efficiency of some quinazoline derivatives on stainless steel 304 in hydrochloric acid solutions, *Int. J. Corros. Scale Inhib*., 2016, **5**, no. 2, 112–131. doi: 10.17675/2305-6894-2016-5-2-2
29. V. Johnsirani, S. Rajendran, A.C.C. Mary, R.J. Rathish, T. Umasankareswari and J. Jeyasundari, Corrosion inhibition by dyes from plants, *Int. J. Nano Corr. Sci. Eng*., 2015, **2**, no. 3, 22–28.
30. N.R. Devi, N. Karthiga, R. Keerthana, T. Umasankareswari, A. Krishnaveni, G. Singh and S. Rajendran, Extracts of leaves as corrosion inhibitors – An overview and corrosion inhibition by an aqueous extract of henna leaves (*Lawsonia inermis*), *Int. J. Corros. Scale Inhib*., 2020, **9**, no. 4, 1169–1193. doi: 10.17675/2305-6894-2020-9-4-2

31. B.A. Farzana and K.R. Ahamed, Mild steel corrosion inhibition by aqueous leaves extract of Scoparia dulcis in acid medium, *World J. Pharm. Res*., 2017, **7**, no. 1, 1094–1108.
32. P.N. Devi, J. Sathiyabama and S. Rajendran, Study of surface morphology and inhibition efficiency of mild steel in simulated concrete pore solution by lactic acid-Zn^{2+} system, *Int. J. Nano Corr. Sci. Engg*., 2017, **6**, no. 1, 18–31.
33. D. Lakshmi, S. Rajendran and J. Sathiyabama, Application Of Infra-Red Spectroscopy In Corrosion Inhibition Studies, *Int. J. Nano Corr. Sci. Engg*., 2016, **3**, no. 4, 181–203.
34. D. Lakshmi, J. Sathiyabama and S. Rajendran, The inhibition effect of o-nitrophenol and Zn^{2+} system on corrosion of aluminium, *Int. J. Corros. Scale Inhib*., 2017, **6**, no. 3, 240–261. doi: 10.17675/2305-6894-2020-9-4-2
35. A.M. Nagiub, H.F.Y. Khalil, M.H. Mahross, B.N.A. Mahran, and M.M.B. El-Sabbah, Beet Root Extract as a Corroison Inhibitor for Mild Steel in 1.0 M HCl Solution, *Int. J. Scient. Engg. Resear*., 2016, **7**, no. 6, 656–663
36. R.M. Silverstein, G.C. Bassler and T.C. Morrill, *Spectrometric Identification of Organic Compounds*, John Wiley & Sons, New York, 1986. 95.
37. I. Sekine and Y. Hirakawa, Effect of 1-Hydroxyethylidene-1, 1-Diphosphonic Acid on the Corrosion of SS 41 Steel in 0.3% Sodium Chloride Solution, *Corrosion*, 1986, **42**, no. 5, 272–277. doi: 10.5006/1.3584904
38. J. Telegdi, *N*-Substituted unusual amino acids as corrosion inhibitors. Part IV: *N*-Acyl derivatives of unnatural amino acids with double bond, *Int. J. Corros. Scale Inhib*., 2016, **5**, no. 4, 360–366. doi: 10.17675/2305-6894-2016-5-4-6
39. M. Banu, R. Joany and S. Rajendran, Green approach to corrosion inhibition of mild steel in acid medium by aqueous extract of Pedalium murex L. Leaves, *Der Pharma Chemica*, 2018, **10**, 21–28.
40. K.R. Ahameda, B.A. Farzanaa, S.J. Diraviama, R. Dorothyb, S. Rajendranb and A. Al-Hashem, Mild Steel Corrosion Inhibition by the Aqueous Extract of Commelina benghalensis Leaves, *Port. Electrochim. Acta*, 2019, **37**, no. 1, 51–70. doi: 10.4152/pea.201901051
41. N.V. Tsirulnikova, Ya.V. Bolt, E.S. Dernovaya, B.N. Driker and T.S. Fetisova, Creation and study of formulations as inhibitors of metal corrosion and scaling for stabilization water treatment in water utilization systems (a review), *Int. J. Corros. Scale Inhib*., 2016, **5**, no. 1, 66. doi: 10.17675/2305-6894-2016-5-1-6
42. W. Liu, A. Singh, Y. Lin, E.E. Ebenso, L. Zhou and B. Huang, 8-Hydroxyquinoline as an Effective Corrosion Inhibitor for 7075 Aluminium Alloy in 3.5% NaCl Solution, *Int. J. Electrochem. Sci*., 2014, **9**, no. 10, 5574–5584.

♦ ♦ ♦